


Cite this: *RSC Adv.*, 2023, 13, 29070

EGFR and PI3K/m-TOR inhibitors: design, microwave assisted synthesis and anticancer activity of thiazole–coumarin hybrids†

Rasha Z. Batran,^a Eman Y. Ahmed,^b Hanem M. Awad,^b Korany A. Ali^c and Nehad A. Abdel Latif^{*a}

A series of thiazoline and thiazolidinone-based 4-hydroxycoumarin derivatives were synthesized using both conventional synthesis procedures and microwave-assisted techniques. The new compounds were evaluated for their cytotoxic effect against three human cancer cell lines; MCF-7, HCT-116 and HepG2 and one normal human cell line (BJ-1). The promising anti-proliferative compounds **2a**, **2b**, **6a** and **6b** were assessed for inhibiting EGFR and PI3K/mTOR. Compound **6a** showed the highest inhibition activity towards the signaling pathway. The apoptotic effect and cell cycle arrest potential of derivative **6a** were examined. Moreover, the molecular docking, physicochemical properties and pharmacokinetic parameters of the promising compound were investigated, as well.

Received 24th May 2023
Accepted 26th September 2023

DOI: 10.1039/d3ra03483f

rsc.li/rsc-advances

1. Introduction

Cancer is a disease of a multifactorial nature that ranks as the second leading cause of death worldwide, resulting in about 10 million deaths in 2020.¹ It has been noted that a number of signaling pathways when dysregulated are subsequently involved in cancer pathogenesis. The PI3K/AKT/mTOR pathway is an intracellular signaling pathway related to a number of biological processes such as apoptosis, cell proliferation and angiogenesis. Dysregulation of this pathway is associated with a vast disturbance in cell growth, survival and metastasis which results in cancer development. Somatic mutations or gaining and losing of key genes are among the factors affecting this pathway in a number of different tumors such as breast, colon and liver cancers.^{2–4}

PI3K/AKT/mTOR pathway is initially activated by the binding of extracellular growth factors to epidermal growth factor receptor (EGFR), then phosphatidylinositol 3-kinase (PI3K) is activated which consequently activates the serine/threonine protein kinase B (PKB/AKT). This leads to some downstream effects as the activation of mechanistic target of rapamycin (mTOR). Agents that target the regulators in this pathway are either single PI3K, AKT or mTOR inhibitors or dual inhibitors of PI3K and mTOR. In theory, inhibiting EGFR and PI3K/mTOR

would probably lead to the strongest inhibition of the whole PI3K/Akt/mTOR pathway.^{5,6}

Coumarin as a privileged heterocyclic ring that displays multifarious biological activities has been utilized to design useful antitumor compounds.^{7–12} A closer look at the coumarin chemical structure and physicochemical properties reveals that the 2H-chromen-2-one ring is planar and lipophilic, which grants the scaffold the ability to interact with a variety of biological counterparts, whereas, the lactone group of the coumarin enable the molecule to form strong polar bonds and to acylate different protein targets.¹³ On the other hand, the thiazole ring is a versatile moiety that demonstrated many desirable biological activities, dabrafenib is an example of a thiazole drug that underwent clinical trials for its selectivity towards tyrosine kinase inhibition.^{14,15} Moreover, thiazoles are reported as potent anticancer agents that are capable of targeting certain kinase pathways, *e.g.* compound **I**, Fig. 1.¹⁶

In an attempt to pursue new antitumor agents, considering the aforementioned information, and as a continuation to our research work in cancer field,^{17–26} the target compounds were rationally developed by using one of the FDA approved drugs that inhibits EGFR (pelitinib) and another that is developed by Novartis and involved in PI3K/AKT/mTOR signaling pathway (NVP-BEZ235) as models, replacing their biologically active quinoline ring with its bioisostere coumarin scaffold, and hybridizing the scaffold with the bioactive thiazole moiety, Fig. 1.

2. Results and discussion

2.1. Chemistry

The target thiazolines and thiazolidinones were prepared from the intermediate thiosemicarbazones **2a–c** through the reaction

^aChemistry of Natural Compounds Department, Pharmaceutical and Drug Industries Research Institute, National Research Centre, Dokki, Cairo, 12622, Egypt. E-mail: eyam_ha@yahoo.com; nehad_km@yahoo.com

^bTanning Materials and Leather Technology Department, National Research Centre, Dokki, Cairo, 12622, Egypt

^cApplied Organic Chemistry Department, Advanced Materials and Nanotechnology Group, National Research Centre, Dokki, Cairo, 12622, Egypt

† Electronic supplementary information (ESI) available. See DOI: <https://doi.org/10.1039/d3ra03483f>



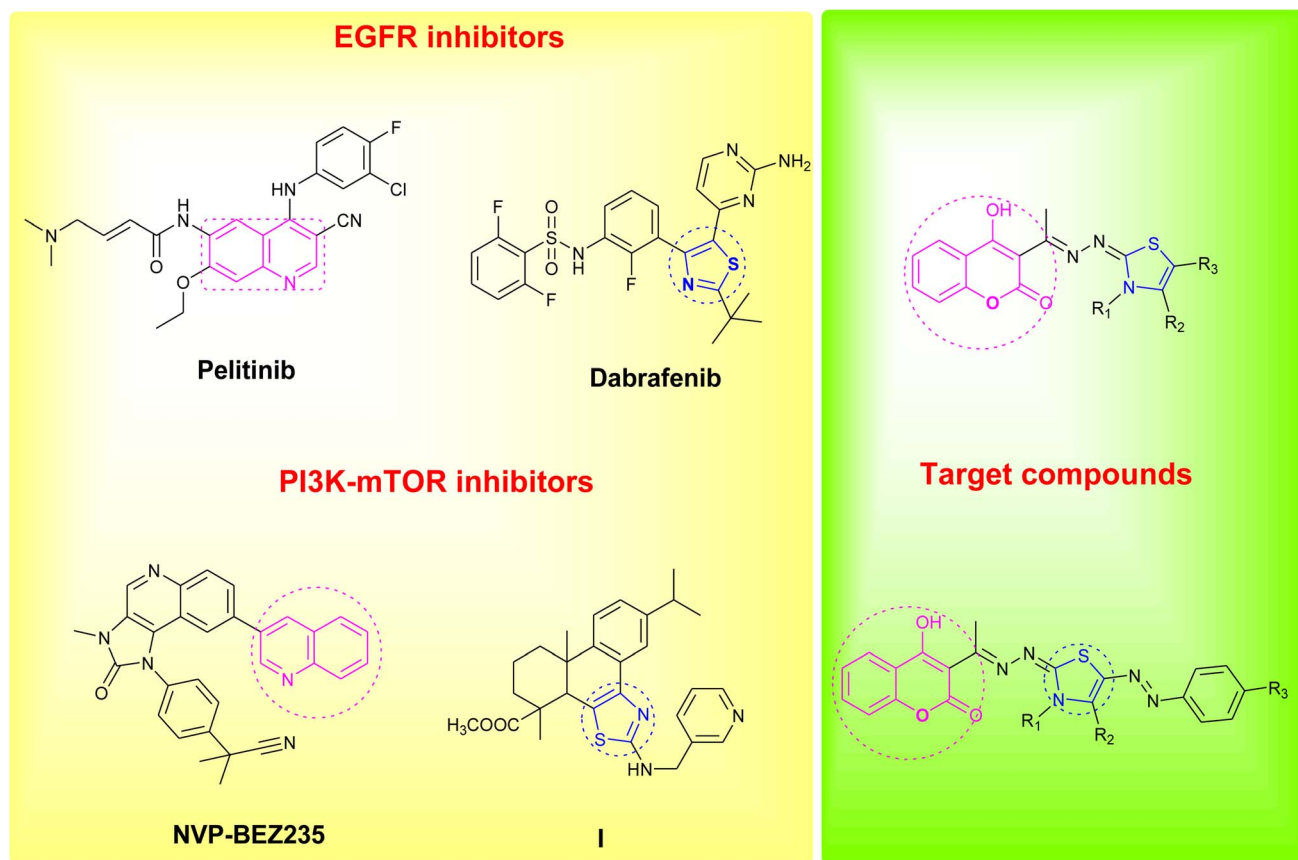
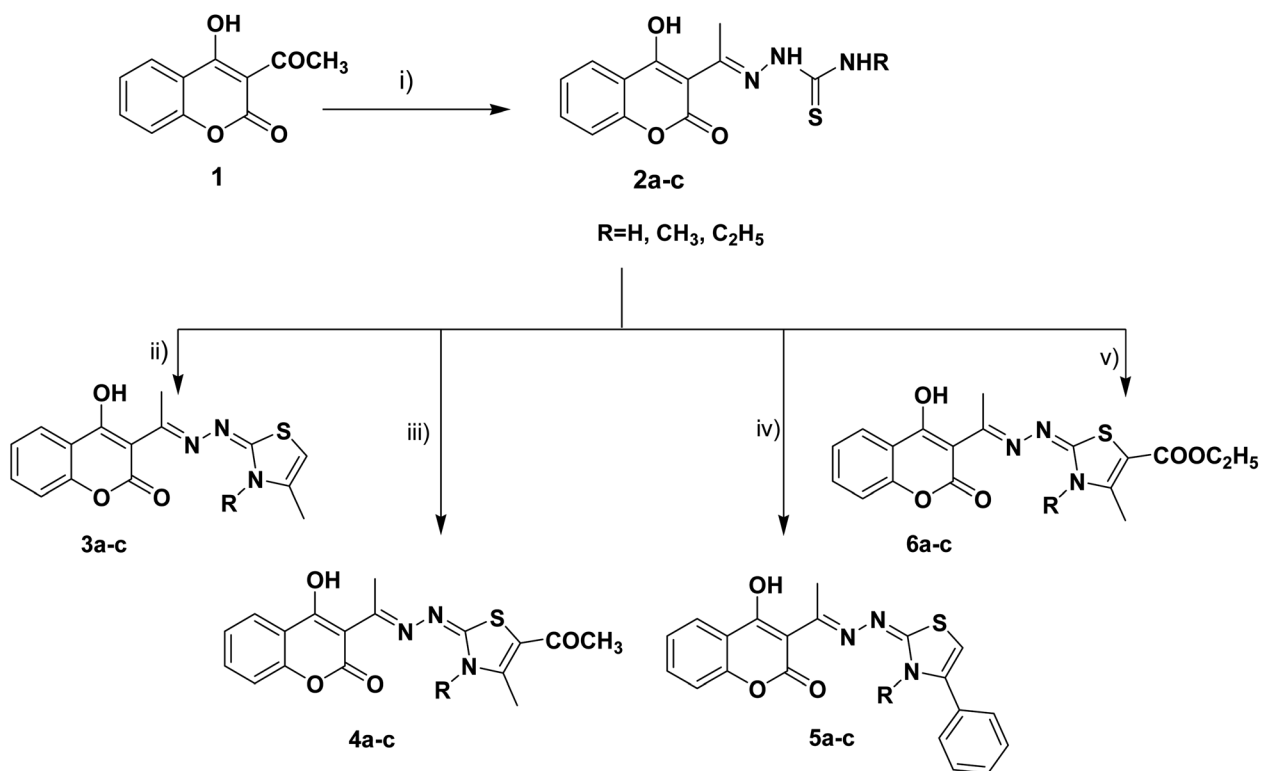
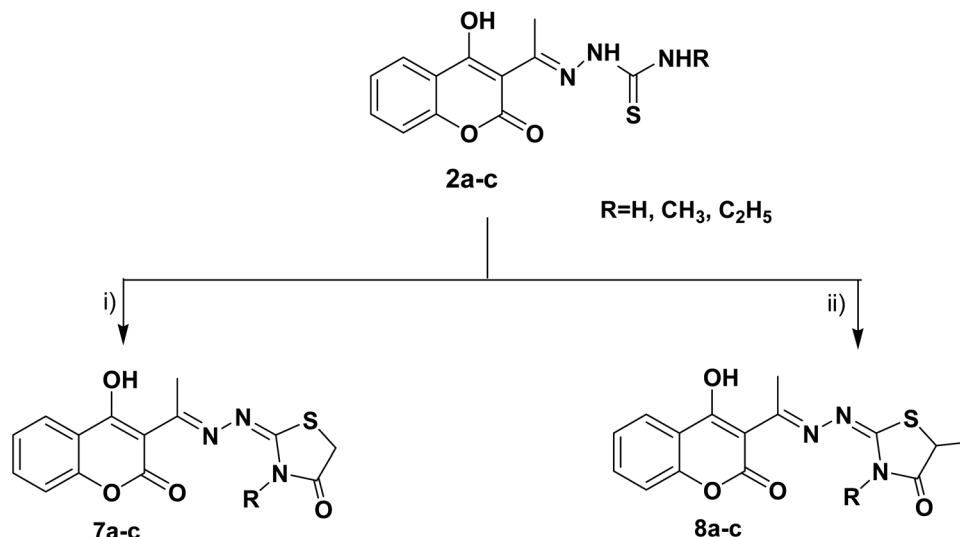


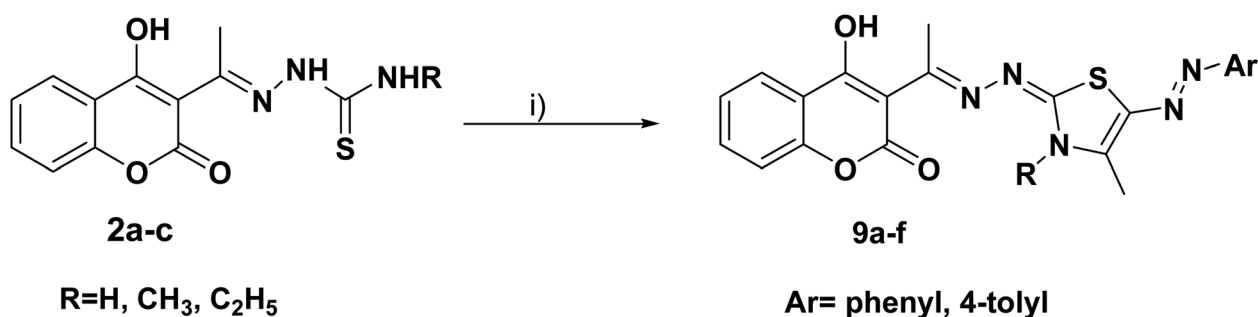
Fig. 1 Reported EGFR and PI3K/mTOR inhibitors and design of the newly synthesized coumarin derivatives.



Scheme 1 Reagents and conditions: (i) $\text{NH}_2\text{NHCSNHR}$, EtOH, AcOH, reflux, (ii) $\text{CH}_3\text{COCH}_2\text{Cl}$, CH_3COONa , EtOH, reflux, (iii) $\text{CH}_3\text{COCH}(\text{Cl})\text{COCH}_3$, CH_3COONa , EtOH, reflux, (iv) PhCOCH_2Br , CH_3COONa , EtOH, reflux, (v) $\text{CH}_3\text{COCH}(\text{Cl})\text{COOC}_2\text{H}_5$, CH_3COONa , EtOH, reflux.



Scheme 2 Reagents and conditions: (i) $CH_3CH_2OCOCH_2Br$, CH_3COONa , EtOH, reflux, (ii) $CH_3CH(Br)COOC_2H_5$, CH_3COONa , EtOH, reflux.



Scheme 3 Reagents and conditions: (i) $CH_3COCH(Cl)N=N-Ar$, dioxane, $N(C_2H_5)_3$.

with different α -haloketones as outlined in Scheme 1. Thus, cyclocondensation of thiosemicarbazones **2a-c** with chloroacetone and/or 3-chloroacetylacetone in ethanol using a catalytic amount of anhydrous sodium acetate yielded the corresponding 4-methylthiazolines **3a-c** and/or 5-acetyl-4-

methylthiazolines **4a-c**, respectively. While the reaction of **2a-c** with phenacyl bromide afforded the 4-phenylthiazoline congeners **5a-c**. Similarly, the 4-methylthiazole-5-carboxylates **6a-c** were obtained *via* the reaction with ethyl-2-chloroacetoacetate, Scheme 1.

Table 1 Comparative study of microwave assisted methods and conventional methods

Compound no.	Microwave assisted methods					Conventional method	
	Irradiation power (W)	Reaction temperature ($^{\circ}C$)	Pressure (Pa)	Time (min)	Yield (%)	Time (h)	Yield (%)
2a	500	125	15	20	93.9	5	79.1
2b	500	125	15	20	92.7	6	89.1
2c	500	125	15	20	93.1	7	88.8
3a	500	150	15	15	93.5	6	85.2
4c	500	125	15	20	89.1	8	80.3
5b	500	150	15	15	91.6	7	85.4
5c	500	150	15	15	93.7	10	77.2
6a	500	125	15	20	89.8	9	81.5
7a	500	150	15	15	92.2	7	78.2
7b	500	150	15	15	90.1	8	82.6
8c	500	125	15	20	88.2	8	80.8
9b	500	150	15	15	91.3	10	78.8



Table 2 The cytotoxic IC₅₀ values of the compounds according to the MTT assay on MCF-7, HCT-116 and HepG2 cells

2a-c

3-6 a-c

7, 8 a-c

9a-f

					IC ₅₀ (μM) ± SD		
Compound	R	R1	R2	Ar	MCF-7	HCT-116	HepG-2
2a	H	—	—	—	8.1 ± 1.1	17.8 ± 2.1	61.4 ± 5.1
2b	CH ₃	—	—	—	13.6 ± 1.5	7.2 ± 0.6	48.1 ± 3.9
2c	C ₂ H ₅	—	—	—	22.7 ± 2.6	17.8 ± 1.8	46.4 ± 3.6
3a	H	CH ₃	H	—	34.5 ± 3.6	32.6 ± 3.1	42.5 ± 4.1
3b	CH ₃	CH ₃	H	—	34.9 ± 3.1	27.2 ± 2.9	46.1 ± 3.7
3c	C ₂ H ₅	CH ₃	H	—	36.5 ± 4.2	36.3 ± 3.5	68.2 ± 5.6
4a	H	CH ₃	COCH ₃	—	25.6 ± 3.1	31.4 ± 3.1	48.8 ± 3.1
4b	CH ₃	CH ₃	COCH ₃	—	32.7 ± 3.5	24.3 ± 2.7	57.1 ± 4.3
4c	C ₂ H ₅	CH ₃	COCH ₃	—	33.7 ± 3.2	38.9 ± 3.2	62.5 ± 3.9
5a	H	Ph	H	—	34.8 ± 4.6	31.8 ± 3.2	47.6 ± 4.1
5b	CH ₃	Ph	H	—	34.6 ± 2.9	42.4 ± 4.1	66.4 ± 5.6
5c	C ₂ H ₅	Ph	H	—	25.9 ± 2.3	9.9 ± 0.9	86.9 ± 5.9
6a	H	CH ₃	COOC ₂ H ₅	—	6.4 ± 0.5	20.4 ± 1.9	57.2 ± 4.3
6b	CH ₃	CH ₃	COOC ₂ H ₅	—	11.2 ± 1.1	5.9 ± 0.7	41.4 ± 2.9
6c	C ₂ H ₅	CH ₃	COOC ₂ H ₅	—	20.7 ± 2.1	24.7 ± 1.6	45.1 ± 4.1
7a	H	H	—	—	26.3 ± 4.1	9.5 ± 1.1	97.6 ± 8.2
7b	CH ₃	H	—	—	32.8 ± 3.5	41.2 ± 3.9	65.7 ± 5.1
7c	C ₂ H ₅	H	—	—	24.2 ± 3.7	10.8 ± 1.1	93.8 ± 6.1
8a	H	CH ₃	—	—	27.4 ± 1.9	38.3 ± 4.2	42.4 ± 3.5
8b	CH ₃	CH ₃	—	—	26.1 ± 3.5	44.8 ± 4.5	67.2 ± 4.9
8c	C ₂ H ₅	CH ₃	—	—	7.4 ± 0.9	44.9 ± 4.3	80.2 ± 5.9
9a	H	—	—	Ph	33.4 ± 2.8	33.9 ± 2.8	71.2 ± 5.1
9b	CH ₃	—	—	Ph	32.3 ± 3.5	37.9 ± 2.5	64.1 ± 5.5
9c	C ₂ H ₅	—	—	Ph	32.8 ± 2.8	47.2 ± 4.5	60.9 ± 4.8
9d	H	—	—	4-CH ₃ Ph	26.3 ± 2.5	45.6 ± 4.2	57.2 ± 4.6
9e	CH ₃	—	—	4-CH ₃ Ph	23.3 ± 1.9	55.2 ± 5.1	74.4 ± 5.9
9f	C ₂ H ₅	—	—	4-CH ₃ Ph	17.8 ± 1.1	40.1 ± 4.7	82.1 ± 6.1
Doxorubicin	—	—	—	—	16.7 ± 1.5	21.8 ± 2.9	63.2 ± 5.8

Furthermore, the heterocyclization of the intermediate thiosemicarbazones **2a–c** with ethyl bromoacetate and/or ethyl-2-bromopropionate under the same reaction conditions gave the corresponding thiazolidinones **7a–c** and 5-methylthiazolidinones **8a–c** respectively, Scheme 2.

Furthermore, the target compounds **9a–f** were prepared *via* reacting the thiosemicarbazones **2a–c** with hydrazonoyl chlorides in dioxane in alkaline medium, Scheme 3. The chemical structures of the synthesized target compounds were confirmed using elemental and spectral analyses (Experimental section).

Synthesis was carried out using conventional synthesis procedures and reactions were modified to improve the yield

and purity of products *via* microwave-assisted techniques. In order to study the effect of different reaction conditions on the products, microwave-assisted synthesis for the derivatives **2a–c**, **3a**, **4c**, **5b**, **5c**, **6a**, **7a**, **7b**, **8c** and **9b** was also carried out using the same reactants with the same molar ratios by condensation of the key intermediates **2a–c** and the corresponding α -halo-ketones in ethanol under heating and pressure conditions, Table 1.

Based on the results outlined in Table 1, it is clear that the microwave irradiation approach provided products with excellent yields (88.2–93.9%) in a short time (15–20 minutes) compared to the classical synthetic methods. This can be



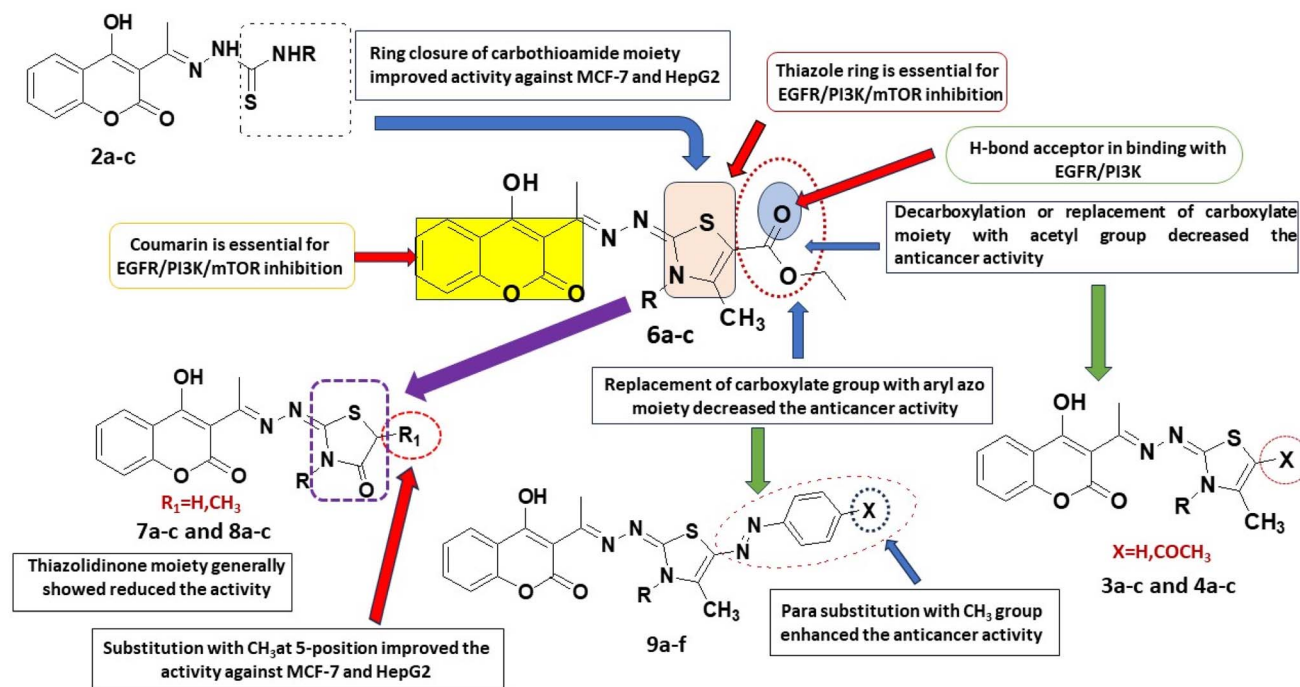


Fig. 2 Structure activity relationship: showing the important bioactive moieties of the most potent compounds 6a–c and comparing compounds 6a–c with compounds 2a–c, 3a–c, 4a–c, 7a–c, 8a–c and 9a–c.

explained by the fact that microwave heating increases the collision of reactants with each other and the high pressure conditions make the distances between the molecules of the reactants closer.

2.2. Biology

2.2.1. Antiproliferative activity. All the target compounds were assessed for their cytotoxic effects on MCF-7 breast adenocarcinoma, HCT-116 colorectal carcinoma, HepG2 liver carcinoma and BJ-1 normal skin fibroblast cell lines using MTT assay. The percentages of intact cells were calculated and compared to those of the control. Activities of these compounds against the three carcinoma cell lines were compared to the activity of doxorubicin. Generally, all the synthesized target compounds suppressed cancer cells in a dose-dependent manner and showed considerable cytotoxic effectiveness against MCF-7 (IC_{50} = 6.4–36.5 μ M vs. 16.7 μ M for doxorubicin) and HCT-116 (IC_{50} = 5.9–55.2 μ M vs. 21.8 μ M for doxorubicin), while they exerted moderate effect against HepG2 (IC_{50} = 41.4–97.6 μ M vs. 63.2 μ M for doxorubicin). All compounds were tested against BJ-1 non-tumor cell line and didn't show any cytotoxicity at the highest concentration (100 μ M) used in this assay.

In case of MCF-7 human breast cancer cells, five compounds (6a, 8c, 2a, 6b and 2b, respectively) have significantly more potent cytotoxic activities than the standard doxorubicin (IC_{50} = 6.4–13.6 μ M vs. 16.7 μ M for doxorubicin), three compounds 9f, 6c and 2c showed remarkable cytotoxic activity (IC_{50} = 17.8, 20.7 and 22.7 μ M, respectively); the rest of the compounds displayed lower cytotoxic activity against MCF-7 relative to the reference drug, Table 2. When the target compounds were examined

against HCT-116 human colorectal carcinoma cells, it was shown that five compounds 6b, 2b, 7a, 5c and 7c have significantly more cytotoxic activities than doxorubicin (IC_{50} = 5.9–10.8 μ M vs. 21.8 μ M for doxorubicin); three compounds 2a, 2c and 6a have comparable potent cytotoxic activities to doxorubicin (IC_{50} = 17.8, 17.8 and 20.4 μ M, respectively) and compounds 4b, 6c and 3b were slightly less active relative to the standard drug (IC_{50} = 24.3, 24.7 and 27.2 μ M, respectively). As for the activity of the synthesized compounds on HepG2 human liver cancer cells, it was found that twelve compounds 6b, 8a, 3a, 6c, 3b, 2c, 5a, 2b, 4a, 4b, 6a, and 9d showed significant more potent cytotoxic activities than the reference drug (IC_{50} = 41.4–57.2 μ M vs. 63.2 μ M for doxorubicin), three compounds 9c, 2a, and 4c (IC_{50} = 60.9, 61.4 and 62.5 μ M, respectively) have equipotent cytotoxic activities to doxorubicin and five compounds 9b, 7b, 5b, 8b and 3c (IC_{50} = 64.1–68.2 μ M) have reasonable cytotoxic activity against HepG2 relative to that of doxorubicin.

Table 3 IC_{50} values of the promising compounds against EGFR/PI3K/mTOR signaling pathway

Compounds	IC_{50} (μ M)		
	EGFR	m-TOR	PI3K
2a	0.311 \pm 0.02	1.388 \pm 0.08	0.174 \pm 0.01
2b	2.275 \pm 0.14	2.957 \pm 0.18	1.331 \pm 0.074
6a	0.184 \pm 0.01	0.719 \pm 0.04	0.131 \pm 0.007
6b	0.563 \pm 0.03	1.449 \pm 0.08	0.361 \pm 0.02
Erlotinib	0.088 \pm 0.005	—	—
Rapamycin	—	0.396 \pm 0.02	—
LY294002	—	—	0.038 \pm 0.002



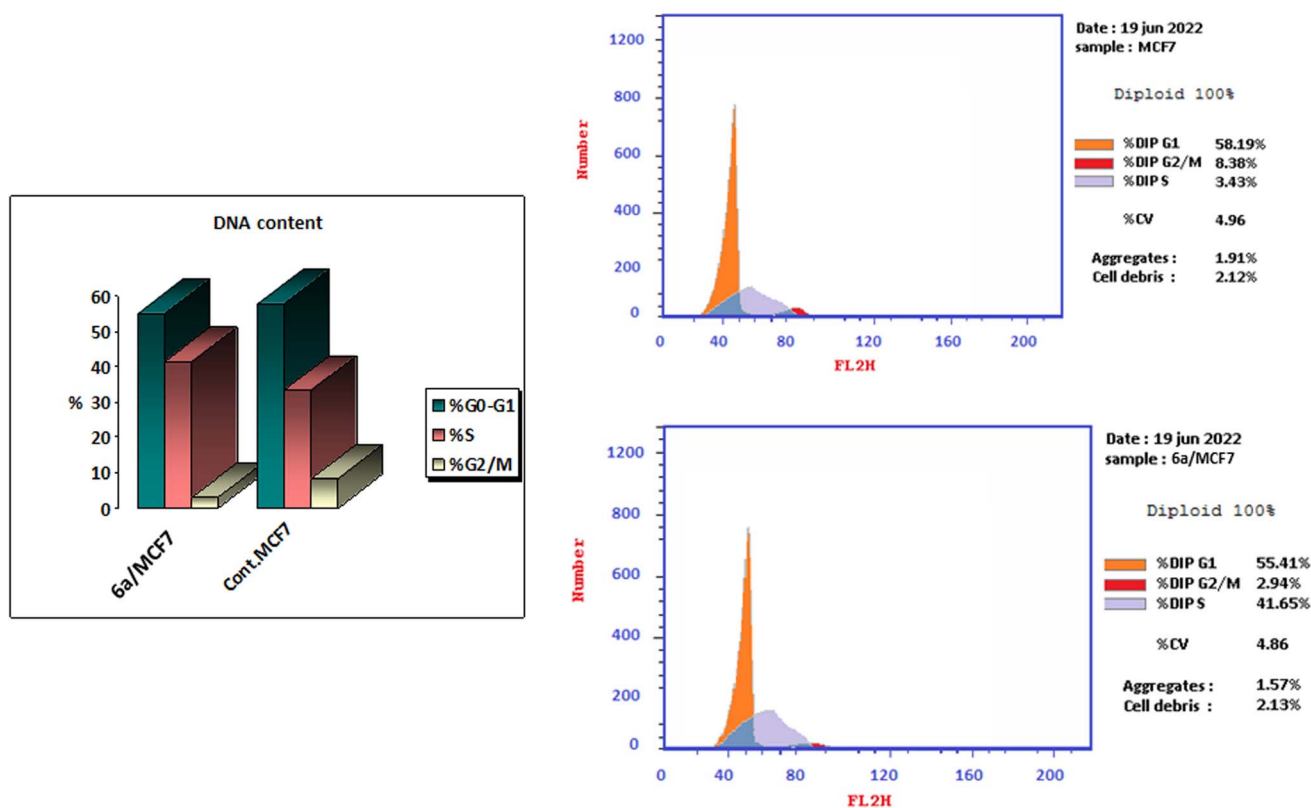


Fig. 3 Cell cycle analysis of MCF-7 after incubation with compound 6a for 48 h.

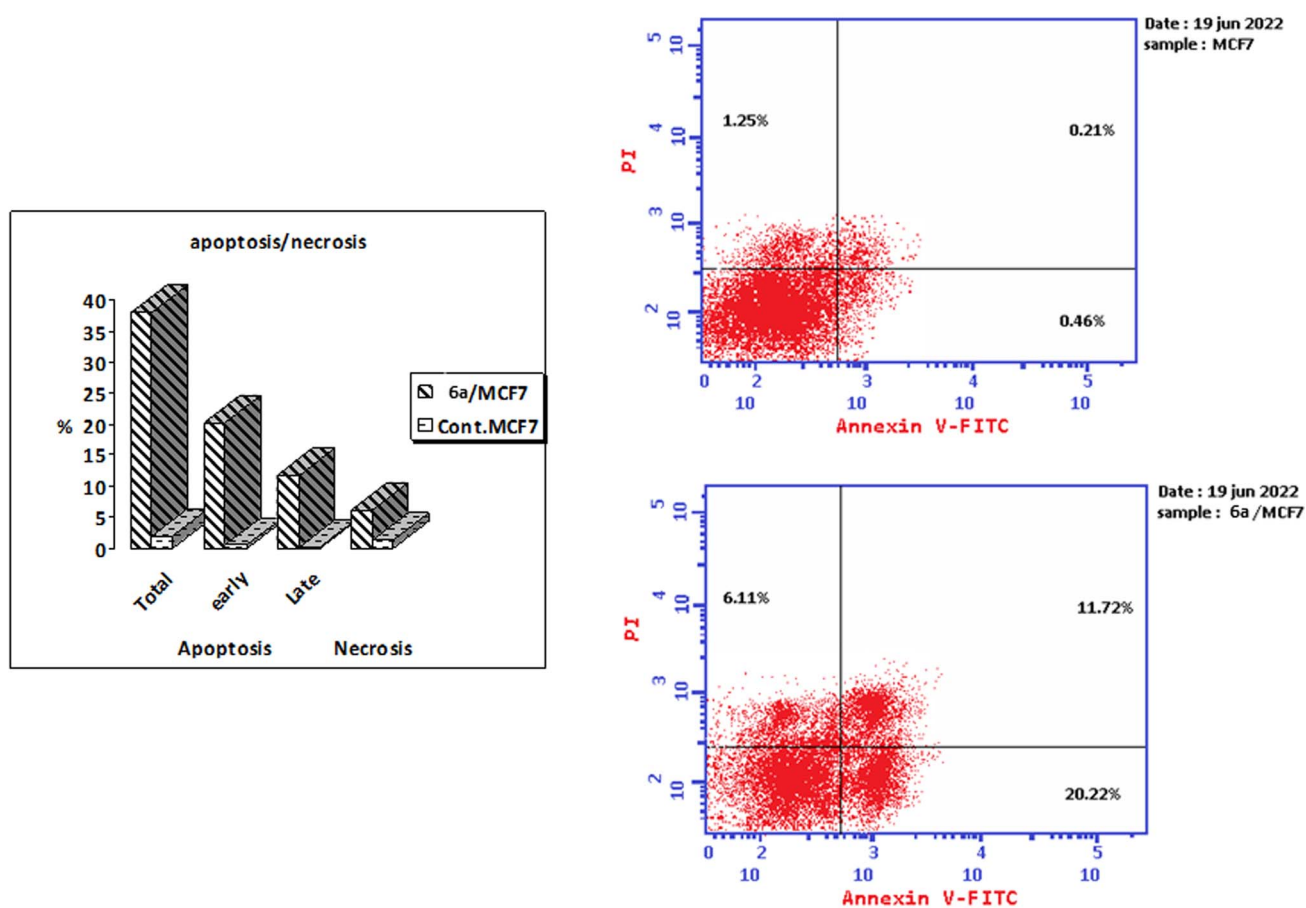


Fig. 4 Induction of apoptosis by compound 6a. Cells were exposed to compound 6a for 48 hours and analyzed by annexin V/PI staining.





Fig. 5 2D interaction diagram showing the co-crystallized ligand docking pose interactions with the key amino acids in EGFR binding site (PDB: 1M17).

From the above results, one can conclude that the six compounds **2a–c** and **6a–c** are non-selectively active on all the three human cancer types. Two compounds (**3b** and **4b**) are active on both human colon cancer HCT-116 and liver cancer cells HepG2 but less active on human breast cancer type. Five compounds (**3a**, **4a**, **5a**, **8a**, and **9d**) are selectively active on only human liver cancer type but less active on both the human breast MCF-7 and human colon HCT-116 cancer types. Two

compounds (**8c**, **9f**) are selectively active on only human breast cancer type MCF-7 but not active on both human colon HCT-116 and liver HepG2 cancer types. Three compounds (**5c**, **7a**, and **7c**) are selectively active on only human colon cancer type HCT-116 but not active on the human liver HepG2 and much less active against breast MCF-7 cancer types.

2.2.2. Structure activity relationship. Compounds **2a**, **2b**, **6a–c**, **8c** and **9f** showed remarkable activity when tested against

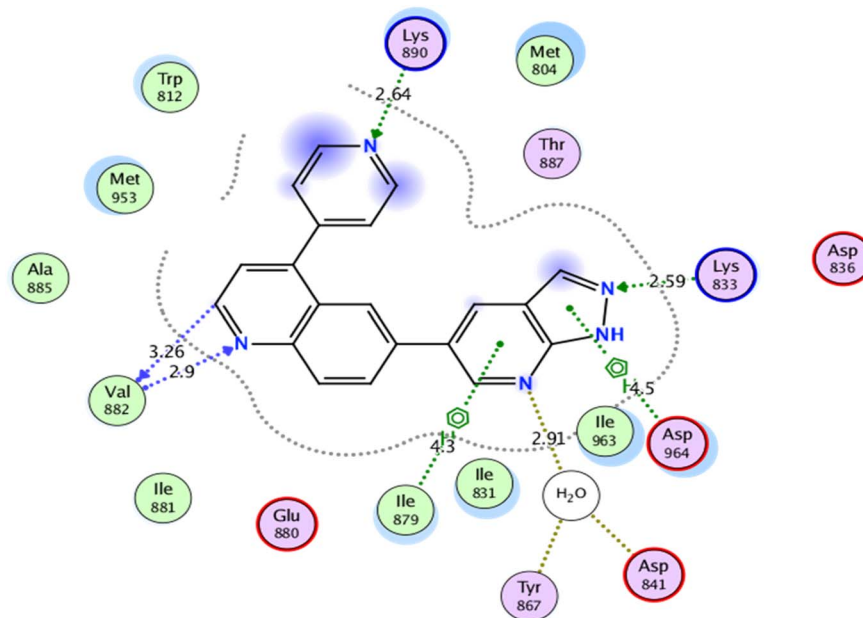


Fig. 6 2D interaction diagram showing the co-crystallized ligand docking pose interactions with the key amino acids in PI3K binding site (PDB: 3L54).



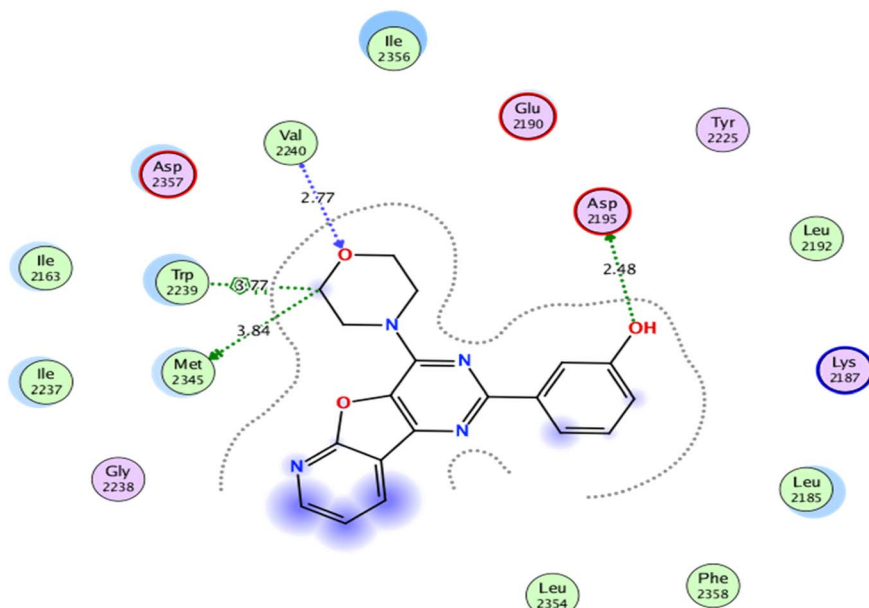


Fig. 7 2D interaction diagram showing the co-crystallized ligand docking pose interactions with the key amino acids in mTOR binding site (PDB: 4JT6).

Table 4 Docking results of compound **6a**

Target protein	Docking score (kcal mol ⁻¹)	Amino acids	Interacting groups	Type of interaction	Bond length (Å)
EGFR	−9.265	Leu694	Coumarin	Arene-H	
		Lys721	O(C=O)CO ₂ C ₂ H ₅	H-bond acceptor	2.40
		Met769	O(C=O)coumarin	H-bond acceptor	2.39
PI3K	−7.320	Lys833	O(C=O)CO ₂ C ₂ H ₅	H-bond acceptor	2.83
		Asp836	(CH ₂)CO ₂ C ₂ H ₅	H-bond donor	2.90
		Val882	O(C=O)coumarin	H-bond acceptor	2.66
		Ile963	Thiazole	Arene-H	
mTOR	−6.855	Trp2239	Coumarin	Arene-arene	
		Trp2239	Coumarin	Arene-arene	
		Val2240	O(C=O)coumarin	H-bond acceptor	2.42
		Asp2357	Thiazole	Arene-H	

MCF-7 breast cancer cell line (IC_{50} = 6.4–20.7 μ M). The 4-methylthiazole-5-carboxylate **6a** was the most potent anti-cancer agent (IC_{50} = 6.4 μ M), it was 2 fold more active than its *N*-methyl congener **6b** (IC_{50} = 11.2 μ M) and 3 times more potent than the *N*-ethyl derivative **6c** (IC_{50} = 20.7 μ M). The *N*-ethyl derivative of 5-methylthiazolidinones **8c** displayed significant cytotoxic potency (IC_{50} = 7.4 μ M) when compared to the *N*-desethyl and *N*-methyl congeners **8a** and **8b** (IC_{50} = 27.4 and 26.1 μ M, respectively). The non-cyclized thiosemicarbazone intermediates **2a–c** showed a pronounced anticancer activity when compared to doxorubicin (IC_{50} = 8.1, 13.6 and 22.7 μ M, respectively). The tolylazo derivatives **9d–f** were more potent than the phenylazo derivatives **9a–c** with compound **9f** being the most active within the arylazo thiazolylidene series (IC_{50} = 17.8 μ M). The thiazolidinone compound **7a** and its *N*-ethyl derivative **7c** showed similar remarkable cytotoxic effects (IC_{50} = 26.28 and 24.17 μ M, respectively). The *N*-ethyl derivative of 4-

phenylthiazoline **5c** showed higher potency (IC_{50} = 25.9 μ M) than the *N*-methyl and *N*-unsubstituted derivatives (IC_{50} ; **5b** = 34.6 μ M, and **5a** = 34.8 μ M, respectively).

For the activity against HCT cancerous cells, compounds **2a–c**, **4b**, **5c**, **6a–c**, **7a** and **7c** showed significant activity when compared to doxorubicin (IC_{50} = 5.9–24.7 μ M). It was noticed that the 3,4-dimethylthiazole-5-carboxylate **6b** and methyl thiosemicarbazone **2b** were the most potent anticancer agents with IC_{50} = 5.9 and 7.2 μ M, respectively compared to doxorubicin (IC_{50} = 21.8 μ M). The thiazolidinone **7a** and its *N*-ethyl congener **7c** as well as the *N*-ethyl derivative of 4-phenylthiazoline **5c** showed high equipotent activity with IC_{50} values of 9.5, 10.8 and 9.9 μ M, respectively. The thiosemicarbazone **2a** and the ethyl-thiosemicarbazone **2c** showed significant equipotent effect (IC_{50} = 17.8 μ M). The thiazole-5-carboxylate **6a** and its *N*-ethyl congener **6c** displayed remarkable anti-HCT effectiveness (IC_{50} = 20.4 and 24.7 μ M, respectively). Moreover, the *N*-methyl



Table 5 Docking results of metabolite of 6a

Target protein	Docking score (kcal mol ⁻¹)	Amino acids	Interacting groups	Type of interaction	Bond length (Å)
EGFR	−9.638	Lys721	−O(COO) [−]	H-bond acceptor	2.44
		Leu768	O(C=O)coumarin	H-bond acceptor	2.98
		Met769	O(C=O)coumarin	H-bond acceptor	2.52
		Thr830	O(C=O)(COO) [−]	H-bond acceptor	2.73
		Asp831	O(C=O)(COO) [−]	H-bond acceptor	2.58
PI3K	−7.720	Lys833	−O(COO) [−]	Ionic	3.00
		Lys833	O(C=O)(COO) [−]	Ionic	2.59
		Lys833	O(C=O)(COO) [−]	H-bond donor	2.59
		Val882	O(C=O)coumarin	H-bond acceptor	2.82
		Asp964	Thiazole	Arene–H	
mTOR	−6.751	Lys2187	O(C=O)(COO) [−]	H-bond acceptor	3.15
		Glu2190	S(thiazole)	H-bond donor	4.15
		Trp2239	Coumarin	Arene–arene	
		Val2240	O(C=O)coumarin	H-bond acceptor	3.28

derivatives of 4-methylthiazoline **3b** (IC₅₀ = 27.2 μM) and 5-acetyl-4-methylthiazoline **4b** (IC₅₀ = 24.3 μM) showed considerable potency higher than their *N*-unsubstituted and *N*-ethyl congeners.

On the other hand, the 3,4-dimethylthiazole-5-carboxylate **6b**, 5-methylthiazolidinone **8a** and 4-methylthiazoline **3a** are the most active derivatives against human liver cancer cell line HepG2 (IC₅₀ = 41.4, 42.4 and 42.5 μM, respectively, *vs.* 63.2 μM for doxorubicin). Compound **6b** was more potent than the *N*-desmethyl derivative **6a** (IC₅₀ = 57.2 μM) and showed equipotent cytotoxicity to its *N*-ethyl congener **6c** (IC₅₀ = 45.1 μM). Within the thiazolidinone series, compound **8a** was the most active (IC₅₀ = 42.4 μM) being more potent than its *N*-alkylated derivatives **8b, c** (IC₅₀ = 67.2 and 80.2 μM, respectively) and its desmethyl congener **7a** (IC₅₀ = 97.66 μM, respectively). The *N*-methyl derivatives of thiazolidinone **7b** and 5-methylthiazolidinone **8b** showed comparable potency to the reference doxorubicin (IC₅₀ = 65.7 and 67.2 μM, respectively, *vs.* 63.2 μM for doxorubicin). The 5-acetyl-4-methylthiazoline **4a** (IC₅₀ = 48.8 μM) and 4-phenyl thiazoline **5a** (IC₅₀ = 47.6 μM) displayed higher cytotoxic activity against HepG2 cells than their *N*-methyl and *N*-ethyl congeners. Moreover, the methyl and ethyl thiosemicarbazones **2b, c** showed remarkable anticancer effect than the unsubstituted thiosemicarbazone **2a** (IC₅₀ = 48.1 and 46.4 μM, respectively, *vs.* 61.4 μM for **2a**). Within the arylazo thiazolidine series, the 4-tolylazo compound **9d** and the phenylazo derivatives **9c** and **9b** were the most active with comparable effect to the reference drug (IC₅₀ = 57.2, 60.9 and 64.1 μM, respectively) (Fig. 2).

2.2.3. In vitro EGFR, m-TOR and PI3K activity assay. Since compounds **2a, 2b, 6a** and **6b** exhibited an excellent cytotoxic activity against MCF-7, HCT-116 and HepG-2 cancer cell lines and at the same time they showed high safety profile towards the chosen human normal cell line, they were selected for further screening on EGFR and PI3K/mTOR. The results of EGFR inhibition assay revealed the promising inhibitory activity of compound **6a** (IC₅₀ = 0.184 μM) compared to the reference erlotinib (IC₅₀ = 0.088 μM), compounds **2a** and **6b** exhibited potent effect with IC₅₀ values 0.311 and 0.563 μM, respectively,

while compound **2b** showed reduced effectiveness against EGFR inhibition (IC₅₀ = 2.275 μM). Similarly, derivative **6a** showed pronounced m-TOR inhibition activity of (IC₅₀ = 0.719 μM)

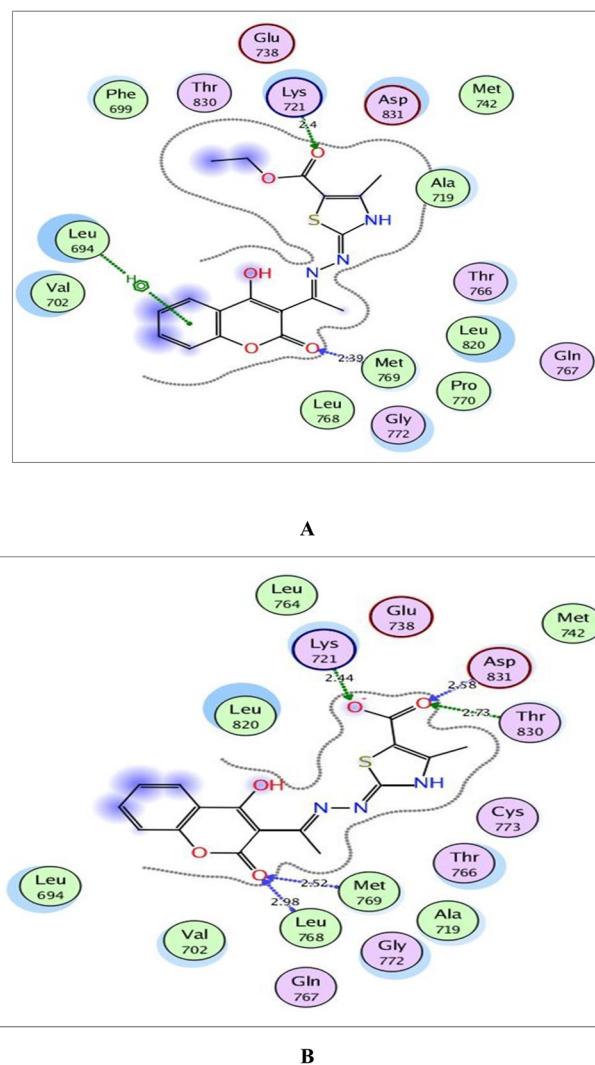


Fig. 8 (A) and (B) Illustrated 2D diagrams of compound **6a** and its metabolite, respectively showing their interactions with the EGFR binding site.



relative to rapamycin as the reference compound which showed an IC_{50} of $0.396\ \mu\text{M}$. Moreover, compounds **2a** and **6b** displayed noticeable equipotent effect against m-TOR ($IC_{50} = 1.388$ and $1.449\ \mu\text{M}$), respectively, while compound **2b** showed less inhibition potency ($IC_{50} = 2.957\ \mu\text{M}$). On the other hand, the selected derivatives **6a** and **2a** exhibited strong comparable PI3K inhibitory activity; at sub-micromolar levels ($IC_{50} = 0.131$ and $0.174\ \mu\text{M}$) versus $0.038\ \mu\text{M}$ for the reference compound LY294002. Compound **2b** exerted considerable PI3K inhibitory activity showing IC_{50} value of $1.331\ \mu\text{M}$. The IC_{50} values of the tested derivatives on EGFR, m-TOR and PI3K were consistent with the promising cytotoxic results (Table 3).

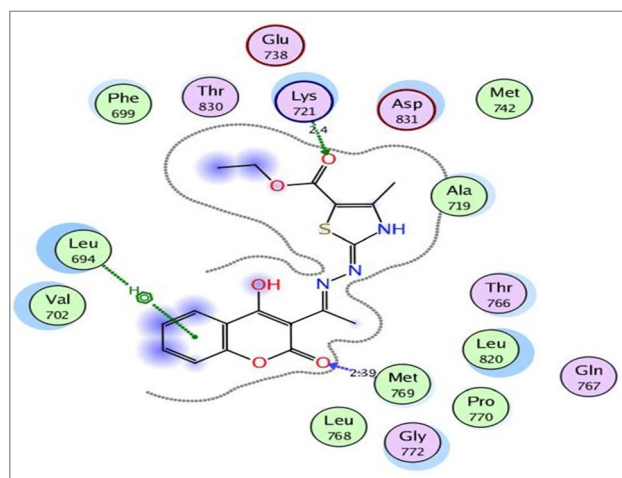
2.2.4. Cell cycle inhibition. Encouraged by the promising cytotoxicity and EGFR/m-TOR/PI3K inhibitory activity of the thiazole derivative **6a**, it was worthy to investigate its effect on cell cycle progression. The results showed that the tested compound inhibited MCF-7 cells proliferation by inducing cell growth arrest at S phase, as shown in Fig. 3.

2.2.5. Cell apoptosis. The effect of the promising derivative **6a** on apoptosis in MCF-7 breast cancer cells was investigated as well. The derivative induced an increase in the early and late cellular apoptosis, Fig. 4.

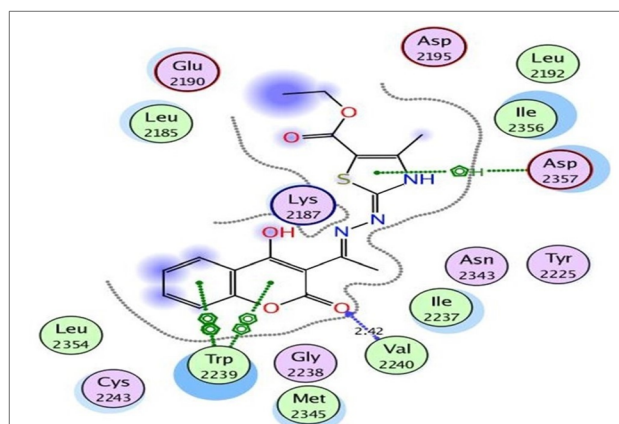
2.3. Molecular docking

In a trial to explore the mode of action of the synthesized derivatives, molecular docking study was performed for the most active compound **6a**. We considered the metabolism of **6a** containing carboxylate group as such; we carried out docking study for its carboxylic acid metabolite as well. Docking setup was first validated by self-docking of the co-crystallized ligand, erlotinib, in the vicinity of the binding site of EGFR showing a binding score of $-10.760\ \text{kcal mol}^{-1}$ and RMSD value of $1.241\ \text{\AA}$, Fig. 5.

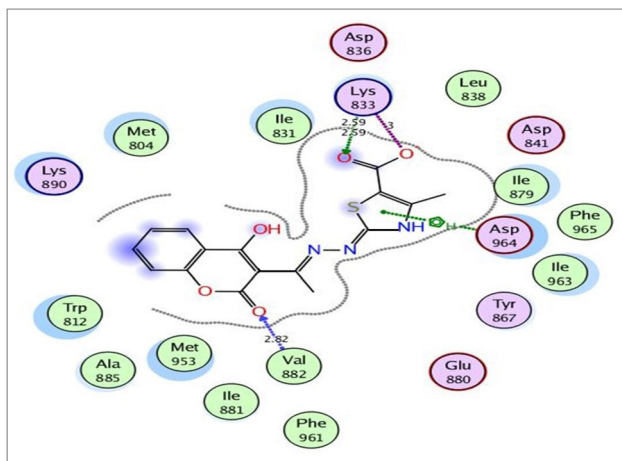
Self-docking of the co-crystallized ligand, 6-(1*H*-pyrazolo[3,4-*b*]pyridin-5-yl)-4-pyridin-4-ylquinoline, in the vicinity of the binding site of PI3K demonstrated a binding score of $-7.511\ \text{kcal mol}^{-1}$ and RMSD value of $0.564\ \text{\AA}$, Fig. 6.



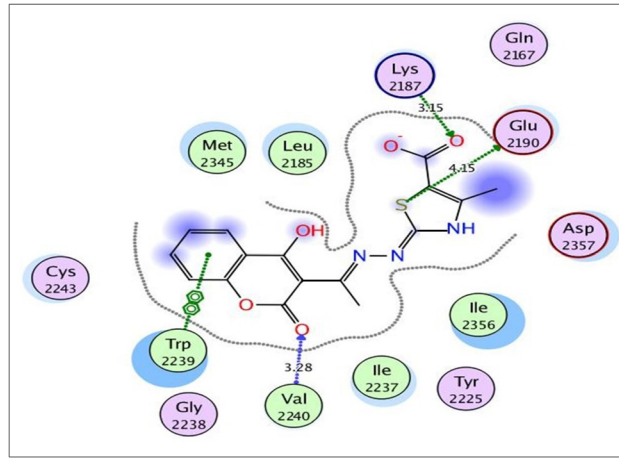
A



A



B



B

Fig. 9 (A) and (B) Illustrated 2D diagrams of compound **6a** and its metabolite, respectively showing their interactions with the PI3K binding site.

Fig. 10 (A) and (B) Illustrated 2D diagrams of compound **6a** and its metabolite, respectively showing their interactions with the mTOR binding site.

Table 6 Physicochemical properties and pharmacokinetics of compound **6a**

Compd	#Rotatable bonds	#H-bond acceptors	#H-bond donors	MR	TPSA	WLOGP
6a	5	7	2	102.19	145.49	2.70
	SOL class	BBB permeant	Lipinski violations	Bioavailability score	PAINS alerts	Synthetic accessibility
	Moderately soluble	No	0	0.55	0	3.79

As for, the self-docking of the co-crystallized ligand, 3-(4-morpholin-4-yl)pyrido[3',2':4,5]furo[3,2-d]pyrimidin-2-yl)phenol, in the vicinity of the binding site of mTOR, a binding score of -7.8611 kcal mol $^{-1}$ and RMSD value of 0.526 Å were recorded, Fig. 7.

The validated setup was then used in predicting the ligand–receptor interactions at the binding site for the compound of interest **6a** and its metabolite. The tested compounds displayed good binding scores and several interactions within the active sites of the target proteins. The results are summarized in Tables 4, 5 and Fig. 8–10.

Regarding the three screened receptors, it was noted that the coumarin scaffold in both **6a** and its metabolite was well fitted through H-bond acceptors between the carbonyl oxygen and the key amino acids Met769 in EGFR, Val882 in PI3K and Val2240 in mTOR, resembling the original ligands (distance: 2.39 & 2.52 Å for EGFR, 2.66 & 2.82 Å for PI3K and 2.42 & 3.28 Å for mTOR, respectively).

By focusing upon EGFR in Fig. 8, the derivative **6a** afforded arene–H interaction between coumarin moiety and Leu694. Also, there is one H-bond between carbonyl oxygen of ethylcarboxylate fragment and Lys721 (distance: 2.40 Å respectively). The metabolized form conserved its fitting through additional H-bonding between carbonyl oxygen of coumarin and the backbone of Leu768 (distance: 2.98 Å). Also, the carboxylate ion formed three H-bonds with Lys721, Thr830 and Asp831 (distance: 2.44, 2.73 and 2.58 Å, respectively).

Within the active site of PI3K, the thiazole moiety displayed arene–H interaction with Ile963 in **6a** and with Asp964 in the metabolite. The ethylcarboxylate fragment in **6a** revealed two H-bonds with the side chains of Lys833 and Asp836 (distance: 2.83 and 2.90 Å, respectively) while carboxylate ion in the metabolite of **6a** showed two ionic bonds and one H-bond with Lys833 (distance: 3.00, 2.59 and 2.59 Å, respectively) (Fig. 9).

Concerning Fig. 10, the coumarin scaffold established arene–arene interactions, two in **6a** and one in its metabolite with Trp2239 within the binding site of mTOR. Also, the thiazole ring shared fixation through arene–H interaction with Asp2357 in **6a** and hydrogen bonding between sulfur atom and the side chain of Glu2190 in the metabolite form. Furthermore, the carboxylate ion in the metabolite of **6a** exhibited H-bond acceptor with Lys2187 (distance: 3.15 Å).

Finally, it could be concluded that the derivative **6a** and its metabolite occupied the same active pockets of EGFR, PI3K and mTOR, as the native ligands. The existence of coumarin and thiazole scaffolds in the structure of **6a** and its metabolite promoted binding through different hydrophobic and hydrophilic interactions. Moreover, the presence of ethylcarboxylate

fragment in **6a** or the carboxylate ion in its metabolite potentiated fixation within the screened receptors.

2.4. *In silico* physicochemical properties, pharmacokinetics parameters and medicinal chemistry friendliness study

Compound **6a** showed moderate solubility profile, with no blood–brain barrier permeation, as well as zero violations of Lipinski's rule and no pain alerts, expressing the main properties of a promising drug-like lead compound, Table 6.

3. Conclusion

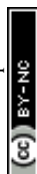
In an attempt to search for new antitumor agents, a series of thiazole based 4-hydroxycoumarin derivatives was designed and synthesized. The primary cytotoxic MTT bioassay against MCF-7, HCT-116 and HepG2 showed that the 4-methylthiazole-5-carboxylates **6a–c** and the thiosemicarbazones **2a–c** were the most potent derivatives against MCF-7 and HCT cells and exhibited pronounced potency against HepG2 with compounds **2a**, **2b**, **6a** and **6b** being the most potent against the three cell lines. Moreover, compound **6a** exhibited the best inhibition of EGFR and PI3K/mTOR. Molecular docking of **6a** and its metabolite showed the importance of coumarin and thiazole moieties for binding interactions within the active sites of EGFR and PI3K/mTOR. Finally, the *in silico* study of the physicochemical properties and pharmacokinetics parameters of **6a** showed that the new derivative is a promising lead compound.

4. Experimental

4.1. Chemistry

All melting points were measured using Electrothermal IA 9000 apparatus and they were uncorrected. NMR spectra were assessed by Bruker 400 MHz spectrometer using TMS as the internal standard. The reactions under microwave irradiation were applied using the STARTSYNTH microwave synthesis lab station (Milestone Srl-Italy). The reactions were applied under 500 W and a pressure of 15 Pa. The reactions were followed by TLC (silica gel, aluminum sheets 60 F254, Merck) using benzene–ethylacetate (7:3 v/v) as eluent. The purity of the synthesized derivatives was determined by elemental analysis and was found to be more than 95%. Compounds **1** and **2a**, **b**, **5a**, **b** and **7a**, **b** were previously prepared.¹⁰

4.1.1. Preparation of 4-(un)substituted-1-(1-(4-hydroxy-2-oxo-2H-chromen-3-yl)ethyl-idenethiosemicarbazides (2a–c). To a solution of 3-acetyl-4-hydroxycoumarin (**1**) (0.51 g, 2.5 mmol) in 20 ml ethyl alcohol, the appropriate thiosemicarbazide compounds; thiosemicarbazide, methyl thiosemicarbazide



and/or ethyl thiosemicarbazide (2.5 mmol) and 0.5 ml glacial acetic acid were added. The reaction mixture was refluxed for 5–7 hours using heating mantle for conventional synthesis and under irradiation power (500 W), reaction temperature (125 °C), pressure (15 Pa) for 20 min using microwave oven for microwave assisted synthesis. The formed precipitate was filtered, dried and recrystallized from acetic acid to yield the target compounds **2a–c**.

4.1.1.1. 4-Methyl-1-(1-(4-hydroxy-2-oxo-2H-chromen-3-yl)ethylidene)thiosemicarbazide (2b). Yellow powder; yield (conventional: 85.2%, microwave: 93.5%); m.p. 210–2 °C; anal. calcd for C₁₃H₁₃N₃O₃S (291.33): C, 53.60; H, 4.50; N, 14.42; S, 11.01. Found: C, 53.69; H, 4.60; N, 14.52; S, 11.08. ¹H NMR (DMSO-*d*₆, δ, ppm): 2.61 (3H, s, CH₃), 2.87, 2.88 (3H, d, CH₃NH), 7.30–8.00 (4H, m, Ar-H), 8.41 (1H, brs, NH, D₂O exchangeable), 10.46 (1H, s, NH, D₂O exchangeable), 15.23 (1H, s, OH, D₂O exchangeable). ¹³C NMR (DMSO-*d*₆, δ, ppm): 17.75, 31.61, 96.93, 116.80, 124.46, 126.07, 134.83, 153.47, 154.67, 165.84, 183.20.

4.1.1.2. Preparation of 3-{1-[(3-(un)substituted-4-methyl-3H-thiazol-2-ylidene)hydrazono]ethyl}-4-hydroxy-2H-chromen-2-ones (3a–c). To a mixture of compounds **2a–c** (2.5 mmol) and chloroacetone (0.2 ml, 2.5 mmol) in absolute ethanol (20 ml), anhydrous sodium acetate (0.41 g, 5 mmol) was added and the reaction mixture was refluxed for 6–10 hours using heating mantle for conventional synthesis and under irradiation power (500 W), reaction temperature (150 °C), pressure (15 Pa) for 15 min using microwave oven for microwave assisted synthesis of **3a**. After cooling, the precipitate was filtered, washed with water, dried, and crystallized from ethanol to give compounds **3a–c**.

4.1.1.2.1. 3-{1-[(4-Methyl-3H-thiazol-2-ylidene)hydrazono]ethyl}-4-hydroxy-2H-chromen-2-one (3a). Buff powder, yield (conventional: 85.2%, microwave: 93.5%); m.p. > 300 °C. Anal. calcd for C₁₅H₁₃N₃O₃S (315.35): C, 57.13; H, 4.16; N, 13.33; S, 10.17. Found: C, 57.19; H, 4.22; N, 13.40; S, 10.25. ¹H NMR (DMSO-*d*₆, δ, ppm): 2.27 (3H, s, CH₃), 2.29 (3H, s, CH₃), 6.63 (1H, s, CH-thiazole), 6.64–8.23 (5H, m, Ar-H and NH), 13.04 (1H, s, OH, D₂O exchangeable). ¹³C NMR (DMSO-*d*₆, δ, ppm): 17.44, 17.61, 100.87, 106.97, 116.70, 117.73, 122.50, 132.75, 133.17, 147.10, 154.16, 156.18, 160.91, 163.12.

4.1.1.2.2. 3-{1-[(3,4-Dimethyl-3H-thiazol-2-ylidene)hydrazono]ethyl}-4-hydroxy-2H-chromen-2-one (3b). Buff powder; yield (82.6%); m.p. 241–2 °C. Anal. calcd for C₁₆H₁₅N₃O₃S (329.37): C, 58.34; H, 4.59; N, 12.76; S, 9.74. Found: C, 58.41; H, 4.66; N, 12.86; S, 9.82. ¹H NMR (DMSO-*d*₆, δ, ppm): 2.20 (3H, s, CH₃), 2.79 (3H, s, CH₃), 3.39 (3H, s, NCH₃), 6.28 (1H, s, CH-thiazole), 7.27–7.99 (5H, m, Ar-H and OH). ¹³C NMR (DMSO-*d*₆, δ, ppm): 14.21, 17.23, 31.84, 95.18, 95.31, 116.61, 119.93, 124.12, 125.63, 133.99, 138.12, 153.34, 161.66, 163.65, 164.33, 177.99.

4.1.1.2.3. 3-{1-[(3-Ethyl-4-methyl-3H-thiazol-2-ylidene)hydrazono]ethyl}-4-hydroxy-2H-chromen-2-one (3c). Yellow powder; yield (87.3%); m.p. 213–4 °C. Anal. calcd for C₁₇H₁₇N₃O₃S (343.4): C, 59.46; H, 4.99; N, 12.24; S, 9.34. Found: C, 59.55; H, 5.09; N, 12.34; S, 9.42. ¹H NMR (DMSO-*d*₆, δ, ppm): 1.25–1.28 (3H, t, CH₃CH₂, *J* = 7.12 Hz), 2.23 (3H, s, CH₃), 2.79 (3H, s, CH₃), 3.89–3.94 (2H, q, CH₂CH₃, *J* = 7.08 Hz), 6.27 (1H, s, CH-

thiazole), 7.28–7.99 (5H, m, Ar-H and OH). ¹³C NMR (DMSO-*d*₆, δ, ppm): 13.24, 13.95, 17.21, 35.04, 95.32, 95.55, 116.63, 119.93, 124.13, 125.65, 134.02, 137.57, 153.35, 161.65, 163.00, 164.43, 178.01.

4.1.3. Preparation of 3-(un)substituted-1-[(5-acetyl-4-methyl-3H-thiazol-2-ylidene)hydrazono]ethyl-4-hydroxy-2H-chromen-2-ones (4a–c). To a mixture of compounds **2a–c** (2.5 mmol) and 3-chloroacetylacetone (0.28 ml, 2.5 mmol) in absolute ethanol (20 ml), anhydrous sodium acetate (0.41 g, 5 mmol) was added and the reaction mixture was refluxed for 7–9 hours. After cooling, the precipitate was filtered, washed with water, dried, and crystallized from ethanol to give compounds **4a–c**.

4.1.3.1. 3-{1-[(5-Acetyl-4-methyl-3H-thiazol-2-ylidene)hydrazono]ethyl}-4-hydroxy-2H-chromen-2-one (4a). Buff powder; yield (86.1%); m.p. > 300 °C. Anal. calcd for C₁₇H₁₅N₃O₄S (357.38): C, 57.13; H, 4.23; N, 11.76; S, 8.97. Found: C, 57.22; H, 4.29; N, 11.83; S, 9.07. ¹H NMR (DMSO-*d*₆, δ, ppm): 2.31 (3H, s, CH₃), 2.46 (3H, s, CH₃), 2.59 (3H, s, COCH₃), 6.79–8.15 (5H, m, Ar-H and NH), 12.79 (1H, s, OH, D₂O exchangeable). ¹³C NMR (DMSO-*d*₆, δ, ppm): 17.34, 18.75, 30.58, 100.27, 107.01, 116.70, 117.86, 122.43, 124.81, 132.54, 133.37, 155.49, 156.16, 160.70, 163.63, 191.10.

4.1.3.2. 3-{1-[(5-Acetyl-3,4-dimethyl-3H-thiazol-2-ylidene)hydrazono]ethyl}-4-hydroxy-2H-chromen-2-one (4b). Buff powder; yield (89.6%); m.p. 250–1 °C. Anal. calcd for C₁₈H₁₇N₃O₄S (371.41): C, 58.21; H, 4.61; N, 11.31; S, 8.63. Found: C, 58.30; H, 4.69; N, 11.38; S, 8.71. ¹H NMR (DMSO-*d*₆, δ, ppm): 2.36 (3H, s, CH₃), 2.47 (3H, s, CH₃), 2.72 (3H, s, COCH₃), 3.37 (3H, s, NCH₃), 7.23–7.96 (5H, m, Ar-H and OH). ¹³C NMR (DMSO-*d*₆, δ, ppm): 14.26, 18.97, 30.08, 32.48, 79.40, 112.74, 113.77, 116.68, 124.60, 125.80, 134.39, 150.72, 158.63, 159.49, 165.50, 167.05, 169.97, 196.78.

4.1.3.3. 3-{1-[(5-Acetyl-3-ethyl-4-methyl-3H-thiazol-2-ylidene)hydrazono]ethyl}-4-hydroxy-2H-chromen-2-one (4c). Buff powder; yield (conventional: 85.2%, microwave: 93.5%); m.p. 277–8 °C. Anal. calcd for C₁₉H₁₉N₃O₄S (385.44): C, 59.21; H, 4.97; N, 10.90; S, 8.32. Found: C, 59.32; H, 5.09; N, 10.99; S, 8.43. ¹H NMR (DMSO-*d*₆, δ, ppm): 1.26–1.30 (3H, t, CH₃CH₂, *J* = 7.04 Hz), 2.46 (3H, s, CH₃), 2.59 (3H, s, CH₃), 2.78 (3H, s, COCH₃), 3.99–4.05 (2H, q, CH₂CH₃, *J* = 7.00 Hz), 7.27–8.03 (5H, m, Ar-H and OH). ¹³C NMR (DMSO-*d*₆, δ, ppm): 13.04, 13.81, 17.36, 29.88, 40.84, 95.90, 97.96, 114.82, 116.60, 124.25, 125.83, 130.10, 134.39, 153.47, 156.74, 161.38, 164.81, 165.67, 195.92.

4.1.4. Preparation of 3-{1-[(3-(un)substituted-4-phenyl-3H-thiazol-2-ylidene)hydrazono]ethyl}-4-hydroxy-2H-chromen-2-ones (5a–c). To a mixture of compounds **2a–c** (2.5 mmol) and phenacyl bromide (0.5 g, 2.5 mmol) in absolute ethanol (20 ml), anhydrous sodium acetate (0.41 g, 5 mmol) was added and the reaction mixture was refluxed for 6–10 hours. After cooling, the precipitate was filtered, washed with water, dried, and crystallized from ethanol to give compounds **5a–c**.

4.1.4.1. 3-{1-[(3-Methyl-4-phenyl-3H-thiazol-2-ylidene)hydrazono]ethyl}-4-hydroxy-2H-chromen-2-one (5b). Yellow powder; yield (conventional: 85.2%, microwave: 93.5%); m.p. 206–7 °C. Anal. calcd for C₂₁H₁₇N₃O₃S (391.44): C, 64.43; H, 4.38; N, 10.73; S, 8.19. Found: C, 64.51; H, 4.42; N, 10.79; S, 8.26. ¹H NMR (DMSO-*d*₆, δ, ppm): 2.82 (3H, s, CH₃), 3.34 (3H, s, NCH₃), 6.62



(1H, s, CH-thiazole), 7.29–8.02 (10H, m, Ar-H and OH). ¹³C NMR (DMSO-*d*₆, δ, ppm): 17.28, 34.03, 95.48, 98.54, 116.62, 119.81, 124.13, 125.66, 129.38, 130.12, 130.27, 134.05, 141.93, 153.35, 161.60, 163.42, 164.95, 178.01.

4.1.5. Preparation of 3-(un)substituted-4-methyl-2-[[1-(4-hydroxy-2-oxo-2H-chromen-3-yl)-ethylidene]-hydrazono]-2,3-dihydro-thiazole-5-carboxylic acid ethyl esters (6a-c). To a mixture of compounds **2a-c** (2.5 mmol) and ethyl-2-chloroacetoacetate (0.35 ml, 2.5 mmol) in absolute ethanol (20 ml), anhydrous sodium acetate (0.41 g, 5 mmol) was added and the reaction mixture was refluxed for 6–10 hours. After cooling, the precipitate was filtered, washed with water, dried, and crystallized from ethanol to give compounds **6a-c**.

4.1.5.1. 4-Methyl-2-[[1-(4-hydroxy-2-oxo-2H-chromen-3-yl)-ethylidene]-hydrazono]-2,3-dihydro-thiazole-5-carboxylic acid ethyl ester (6a). Yellow powder; yield (conventional: 85.2%, microwave: 93.5%); m.p. 289–90 °C. Anal. calcd for C₁₈H₁₇N₃O₅S (387.41): C, 55.80; H, 4.42; N, 10.85; S, 8.28. Found: C, 55.92; H, 4.49; N, 10.93; S, 8.36. ¹H NMR (DMSO-*d*₆, δ, ppm): 1.26–1.29 (3H, t, CH₃ CH₂, *J* = 7.00 Hz), 2.39 (3H, s, CH₃), 2.72 (3H, s, CH₃), 4.18–4.24 (2H, q, CH₂ CH₃, *J* = 7.0 Hz), 6.80–8.00 (5H, m, Ar-H and NH), 12.52 (1H, s, OH, D₂O exchangeable). ¹³C NMR (DMSO-*d*₆, δ, ppm): 14.64, 16.09, 17.42, 60.92, 85.93, 101.74, 116.75, 118.18, 124.60, 132.14, 133.60, 156.00, 156.56, 160.02, 162.79.

4.1.5.2. 3,4-Dimethyl-2-[[1-(4-hydroxy-2-oxo-2H-chromen-3-yl)-ethylidene]-hydrazono]-2,3-dihydro-thiazole-5-carboxylic acid ethyl ester (6b). Yellow powder; yield (87.6%); m.p. 294–5 °C. Anal. calcd for C₁₉H₁₉N₃O₅S (401.44): C, 56.85; H, 4.77; N, 10.47; S, 7.99. Found: C, 57.00; H, 4.85; N, 10.53; S, 8.08. ¹H NMR (DMSO-*d*₆, δ, ppm): 1.28–1.31 (3H, t, CH₃ CH₂, *J* = 7.08 Hz), 2.58 (3H, s, CH₃), 2.80 (3H, s, CH₃), 3.46 (3H, s, NCH₃), 4.23–4.28 (2H, q, CH₂ CH₃, *J* = 7.12 Hz), 7.27–8.04 (5H, m, Ar-H and OH). ¹³C NMR (DMSO-*d*₆, δ, ppm): 13.30, 14.71, 17.37, 32.35, 61.48, 95.78, 100.67, 116.63, 119.43, 124.10, 125.80, 134.35, 149.59, 153.34, 160.18, 161.07, 161.41, 166.83.

4.1.5.3. 3-Ethyl-4-methyl-2-[[1-(4-hydroxy-2-oxo-2H-chromen-3-yl)-ethylidene]-hydrazono]-2,3-dihydro-thiazole-5-carboxylic acid ethyl ester (6c). Orange powder; yield (88.4%); m.p. 205–6 °C. Anal. calcd for C₂₀H₂₁N₃O₅S (415.46): C, 57.82; H, 5.09; N, 10.11; S, 7.72. Found: C, 57.91; H, 5.14; N, 10.18; S, 7.80. ¹H NMR (DMSO-*d*₆, δ, ppm): 1.29–1.31 (6H, m, 2CH₃ CH₂), 2.60 (3H, s, CH₃), 2.78 (3H, s, CH₃), 3.97–4.02 (2H, q, CH₂ CH₃, *J* = 6.72 Hz), 4.24–4.28 (2H, q, CH₂ CH₃, *J* = 7.08 Hz), 7.28–8.03 (5H, m, Ar-H and OH). ¹³C NMR (DMSO-*d*₆, δ, ppm): 12.89, 14.71, 17.29, 39.34, 61.48, 95.76, 100.98, 116.61, 119.41, 124.18, 125.78, 134.30, 148.82, 153.33, 160.18, 161.07, 161.41, 166.83, 178.15.

4.1.6. Preparation of 3-(un)substituted-2-[[1-(4-hydroxy-2-oxo-2H-chromen-3-yl)-ethylidene]-hydrazono]-thiazolidin-4-ones (7a-c). To a mixture of compounds **2a-c** (2.5 mmol) and ethylbromoacetate (0.28 ml, 2.5 mmol) in absolute ethanol (20 ml), anhydrous sodium acetate (0.41 g, 5 mmol) was added and the reaction mixture was refluxed for 7–9 hours. After cooling, the precipitate was filtered, washed with water, dried, and crystallized from ethanol to give compounds **7a-c**.

4.1.6.1. 3-Methyl-2-[[1-(4-hydroxy-2-oxo-2H-chromen-3-yl)-ethylidene]-hydrazono]-thiazolidin-4-one (7b). Yellow powder;

yield (conventional: 85.2%, microwave: 93.5%); m.p. > 300 °C. Anal. calcd for C₁₅H₁₃N₃O₄S (331.35): C, 54.37; H, 3.95; N, 12.68; S, 9.68. Found: C, 54.43; H, 4.02; N, 12.77; S, 9.75. ¹H NMR (DMSO-*d*₆, δ, ppm): 2.82 (3H, s, CH₃), 3.11 (3H, s, NCH₃), 4.23 (2H, s, CH₂-thiazolidinone), 7.31–8.00 (5H, m, Ar-H and OH). ¹³C NMR (DMSO-*d*₆, δ, ppm): 14.47, 29.60, 32.71, 99.15, 117.61, 122.27, 123.77, 126.76, 138.74, 149.72, 157.37, 160.44, 162.36, 163.69, 172.24.

4.1.7. Preparation of 3-(un)substituted-5-methyl-2-[[1-(4-hydroxy-2-oxo-2H-chromen-3-yl)-ethylidene]-hydrazono]-thiazolidin-4-ones (8a-c). To a mixture of compounds **2a-c** (2.5 mmol) and ethyl-2-bromopropionate (0.32 ml, 2.5 mmol) in absolute ethanol (20 ml), anhydrous sodium acetate (0.41 g, 5 mmol) was added and the reaction mixture was refluxed for 7–9 hours. After cooling, the precipitate was filtered, washed with water, dried, and crystallized from ethanol to give compounds **8a-c**.

4.1.7.1. 5-Methyl-2-[[1-(4-hydroxy-2-oxo-2H-chromen-3-yl)-ethylidene]-hydrazono]-thiazolidin-4-one (8a). Yellow powder; yield (87.2%); m.p. 292–3 °C. Anal. calcd for C₁₅H₁₃N₃O₄S (331.35): C, 54.37; H, 3.95; N, 12.68; S, 9.68. Found: C, 54.45; H, 4.05; N, 12.77; S, 9.74. ¹H NMR (DMSO-*d*₆, δ, ppm): 1.60–1.62 (3H, d, CH₃-thiazolidinone, *J* = 7.28 Hz), 2.77 (3H, s, CH₃), 4.51–4.56 (1H, q, CH-thiazolidinone, *J* = 7.20 Hz), 7.31–8.01 (5H, m, Ar-H and NH), 12.34 (1H, s, OH, D₂O exchangeable). ¹³C NMR (DMSO-*d*₆, δ, ppm): 18.91, 19.01, 45.75, 96.15, 116.81, 119.61, 124.43, 125.86, 134.91, 149.55, 153.55, 163.69, 164.86, 176.50.

4.1.7.2. 3,5-Dimethyl-2-[[1-(4-hydroxy-2-oxo-2H-chromen-3-yl)-ethylidene]-hydrazono]-thiazolidin-4-one (8b). Yellow powder; yield (87.9%); m.p. 241–2 °C. Anal. calcd for C₁₆H₁₅N₃O₄S (345.37): C, 55.64; H, 4.38; N, 12.17; S, 9.28. Found: C, 55.72; H, 4.48; N, 12.26; S, 9.37. ¹H NMR (DMSO-*d*₆, δ, ppm): 1.62–1.64 (3H, d, CH₃-thiazolidinone, *J* = 7.20 Hz), 2.81 (3H, s, CH₃), 3.17 (3H, s, NCH₃), 4.51–4.57 (1H, q, CH-thiazolidinone, *J* = 7.12), 7.30–7.99 (5H, m, Ar-H and OH). ¹³C NMR (DMSO-*d*₆, δ, ppm): 17.56, 18.88, 29.99, 44.44, 96.15, 116.82, 119.27, 124.48, 125.87, 134.90, 153.53, 158.91, 161.89, 165.50, 166.70, 174.76.

4.1.7.3. 3-Ethyl-5-methyl-2-[[1-(4-hydroxy-2-oxo-2H-chromen-3-yl)-ethylidene]-hydrazono]-thiazolidin-4-one (8c). Yellow powder; yield (conventional: 85.2%, microwave: 93.5%); m.p. 185–6 °C. Anal. calcd for C₁₇H₁₇N₃O₄S (359.4): C, 56.81; H, 4.77; N, 11.69; S, 8.92. Found: C, 56.89; H, 4.85; N, 11.74; S, 9.01. ¹H NMR (DMSO-*d*₆, δ, ppm): 1.19–1.23 (3H, t, CH₃ CH₂, *J* = 7.12 Hz), 1.62–1.64 (3H, d, CH₃-thiazolidinone, *J* = 7.24 Hz), 2.81 (3H, s, CH₃), 3.74–3.80 (2H, q, CH₂ CH₃, *J* = 7.04 Hz), 4.53–4.59 (1H, q, CH-thiazolidinone, *J* = 7.16 Hz), 7.31–7.99 (5H, m, Ar-H and OH). ¹³C NMR (DMSO-*d*₆, δ, ppm): 12.50, 17.47, 18.92, 38.58, 44.38, 96.14, 116.78, 119.27, 124.38, 125.84, 134.81, 153.52, 157.93, 161.29, 170.57, 174.40, 179.01.

4.1.8. Preparation of 3-(un)substituted-1-[[4-methyl-5-phenylazo-3H-thiazol-2-ylidene]-hydrazono]-ethyl-4-hydroxy-2H-chromen-2-one (9a-f). A mixture of compounds **2a-c** (2.5 mmol) and appropriate hydrazonoyl chlorides (2.5 mmol) in dioxane (20 ml) containing triethylamine (0.25 ml, 1 mmol) was heated under reflux for 8–10 h and then cooled. The solution was poured onto crushed ice and concentrated hydrochloric



acid. The solid produced was collected by filtration and crystallized from the ethanol to give compounds **9a–f**.

4.1.8.1. 3-{1-[(4-Methyl-5-phenylazo-3H-thiazol-2-ylidene)-hydrazono]-ethyl}-4-hydroxy-2H-chromen-2-one (**9a**). Reddish brown powder; yield (78.7%); m.p. 103–5 °C. Anal. calcd for $C_{21}H_{17}N_5O_3S$ (419.46): C, 60.13; H, 4.09; N, 16.70; S, 7.64. Found: C, 60.07; H, 4.01; N, 16.59; S, 7.54. 1H NMR (DMSO- d_6 , δ , ppm): 2.45 (3H, s, CH_3), 2.66 (3H, s, CH_3), 7.26–8.02 (11H, m, Ar-H, OH and NH). ^{13}C NMR (DMSO- d_6 , δ , ppm): 9.00, 12.18, 115.34, 117.26, 119.07, 125.01, 125.26, 125.69, 129.64, 129.85, 130.07, 130.18, 131.07, 137.15, 144.98, 158.20, 159.76, 161.00, 178.38.

4.1.8.2. 3-{1-[(3,4-Dimethyl-5-phenylazo-3H-thiazol-2-ylidene)-hydrazono]-ethyl}-4-hydroxy-2H-chromen-2-one (**9b**). Reddish brown powder; yield (conventional: 85.2%, microwave: 93.5%); m.p. 169–70 °C. Anal. calcd for $C_{22}H_{19}N_5O_3S$ (433.48): C, 60.96; H, 4.42; N, 16.16; S, 7.40. Found: C, 60.85; H, 4.35; N, 16.08; S, 7.31. 1H NMR (DMSO- d_6 , δ , ppm): 2.62 (3H, s, CH_3), 2.69 (3H, s, CH_3), 3.57 (3H, s, CH_3), 7.19–7.96 (10H, m, Ar-H and OH). ^{13}C NMR (DMSO- d_6 , δ , ppm): 17.81, 17.93, 30.16, 116.55, 116.74, 117.27, 123.01, 123.82, 124.05, 125.23, 125.47, 125.75, 126.07, 129.75, 131.85, 137.03, 153.35, 154.31, 154.58, 178.35.

4.1.8.3. 3-{1-[(3-Ethyl-4-methyl-5-phenylazo-3H-thiazol-2-ylidene)-hydrazono]-ethyl}-4-hydroxy-2H-chromen-2-one (**9c**). Reddish brown powder; yield (78.8%); m.p. 126–127 °C. Anal. calcd for $C_{23}H_{21}N_5O_3S$ (447.51): C, 61.73; H, 4.73; N, 15.65; S, 7.17. Found: C, 61.80; H, 4.81; N, 15.74; S, 7.26. 1H NMR (DMSO- d_6 , δ , ppm): 1.36–1.39 (3H, t, CH_3), 2.69 (3H, s, CH_3), 2.79 (3H, s, CH_3), 4.09–4.14 (2H, q, CH_2), 7.26–8.02 (10H, m, Ar-H and OH). ^{13}C NMR (DMSO- d_6 , δ , ppm): 12.54, 17.26, 17.84, 30.05, 116.57, 117.30, 119.29, 122.26, 123.22, 124.13, 124.32, 125.22, 125.68, 129.65, 129.74, 130.04, 137.12, 152.13, 153.29, 161.21, 168.67, 176.89.

4.1.8.4. 3-{1-[(4-Methyl-5-(4-tolyl)azo-3H-thiazol-2-ylidene)-hydrazono]-ethyl}-4-hydroxy-2H-chromen-2-one (**9d**). Reddish brown powder; yield (76.5%); m.p. 145–6 °C. Anal. calcd for $C_{22}H_{19}N_5O_3S$ (433.48): C, 60.96; H, 4.42; N, 16.16; S, 7.40. Found: C, 60.88; H, 4.31; N, 16.06; S, 7.29. 1H NMR (DMSO- d_6 , δ , ppm): 2.39 (3H, s, CH_3), 2.60 (3H, s, CH_3), 2.68 (3H, s, CH_3), 7.17–7.84 (10H, m, Ar-H, OH and NH). ^{13}C NMR (DMSO- d_6 , δ , ppm): 15.71, 17.86, 21.10, 115.36, 116.78, 117.30, 118.43, 122.49, 123.44, 123.56, 125.78, 125.71, 130.06, 130.42, 131.88, 133.77, 141.04, 150.34, 159.55.

4.1.8.5. 3-{1-[(3,4-Dimethyl-5-(4-tolyl)azo-3H-thiazol-2-ylidene)-hydrazono]-ethyl}-4-hydroxy-2H-chromen-2-one (**9e**). Reddish brown powder; yield (74.3%); m.p. 152–3 °C. Anal. calcd for $C_{23}H_{21}N_5O_3S$ (447.51): C, 61.73; H, 4.73; N, 15.65; S, 7.17. Found: C, 61.62; H, 4.64; N, 15.55; S, 7.09. 1H NMR (DMSO- d_6 , δ , ppm): 2.35 (3H, s, CH_3), 2.63 (3H, s, CH_3), 2.74 (3H, s, CH_3), 3.49 (3H, s, CH_3), 7.21–7.97 (9H, m, Ar-H and OH). ^{13}C NMR (DMSO- d_6 , δ , ppm): 9.59, 17.87, 21.11, 25.23, 115.34, 116.92, 117.26, 118.42, 122.30, 123.44, 123.59, 124.66, 126.00, 130.10, 131.55, 135.76, 153.42, 157.46, 161.33, 164.19, 166.71, 168.70.

4.1.8.6. 3-{1-[(3-Ethyl-4-methyl-5-(4-tolyl)azo-3H-thiazol-2-ylidene)-hydrazono]-ethyl}-4-hydroxy-2H-chromen-2-one (**9f**). Reddish brown powder; yield (77.1%); m.p. 159–60 °C. Anal.

calcd for $C_{24}H_{23}N_5O_3S$ (461.54): C, 62.46; H, 5.02; N, 15.17. Found: C, 62.34; H, 5.09; N, 15.06. 1H NMR (DMSO- d_6 , δ , ppm): 1.35–1.39 (3H, t, CH_3), 2.39 (3H, s, CH_3), 2.59 (3H, s, CH_3), 2.66 (3H, s, CH_3), 4.10–4.14 (2H, q, CH_2), 7.26–8.02 (9H, m, Ar-H and OH). ^{13}C NMR (DMSO- d_6 , δ , ppm): 7.44, 11.72, 13.77, 25.45, 34.05, 115.35, 116.78, 117.51, 118.51, 121.59, 123.44, 123.69, 125.73, 127.14, 127.66, 128.00, 130.12, 137.19, 153.35, 154.39, 159.50, 162.91, 164.10, 167.06.

4.2. Biology

4.2.1. MTT anti-proliferative assay. MCF-7 (human breast adenocarcinoma), HCT-116 (human colorectal carcinoma), human liver carcinoma (HepG-2), and the normal human skin fibroblast (BJ-1) cell lines were purchased from the American Type Culture Collection (Rockville, MD, USA) and maintained in Dulbecco's Modified Eagle's Medium (DMEM) supplemented with 10% heat-inactivated fetal bovine serum (FBS), 100 U ml $^{-1}$ penicillin, and 100 U ml $^{-1}$ streptomycin. The cells were grown at 37 °C in a humidified atmosphere of 5% CO $_2$. The anti-proliferative activities were estimated by the 3-(4,5-dimethyl-2-thiazolyl)-2,5-diphenyl-2H-tetrazolium bromide (MTT) assay. This test is based on MTT cleavage by mitochondrial dehydrogenases form viable cells.^{27–29} Cells were placed in a 96 well sterile microplate (5 \times 10 4 cells per well) and incubated at 37 °C in serum-free media containing dimethyl sulfoxide (DMSO) and either a series of various concentrations of each compound or doxorubicin (positive control) for 48 h before the MTT assay. After incubation, the media were removed and 40 μ l MTT (2.5 mg ml $^{-1}$) was added to each well. Incubation was resumed for an additional 4 h. The purple formazan dye crystals were solubilized with 200 μ l DMSO. Absorbance was measured at 590 nm in a Spectra Max Paradigm Multi-Mode microplate reader (Molecular Devices, LLC, San Jose, CA, USA). Relative cell viability was expressed as the mean percentage of viable cells compared to the untreated control cells. All experiments were conducted in technical triplicate and three biological replicates. All values were reported as mean \pm SD. IC $_{50}$ s were determined by SPSS Inc. probit analysis (IBM Corp., Armonk, NY, USA).

4.2.2. In vitro EGFR activity assay. The EGFR kinase activity assay for compounds **2a**, **2b**, **6a** and **6b** was estimated according to the manufacturer procedures, using EGFR kinase assay kit (BPS Bioscience, Cat. #40321). The kit uses Kinase-Glo MAX as the detection reagent (Promega #V6071). Results of the tested compound were assessed by measuring the luminescence using a microplate reader.

4.2.3. In vitro m-TOR activity assay. The assay was conducted for compounds **2a**, **2b**, **6a** and **6b** using the K-LISA TM mTOR Activity Kit which is an ELISA-based assay (Calbiochem kit, Cat. #CBA055) following the manufacturing procedure. The kit utilizes a p70S6K-GST fusion protein as a specific mTOR substrate, where active mTOR phosphorylates p70S6K. The phosphorylated substrate is detected with anti-p70S6K-T389 antibody, followed by detection with HRP-antibody conjugate and TMB substrate and relative activity is determined by reading the absorbance at dual wavelengths of 450/540 nm or 450/595 nm.



4.2.4. *In vitro* PI3K activity assay. The PI3K activity assay was performed for compounds **2a**, **2b**, **6a** and **6b** using the PI3K β (p110 β /p85 α) assay kit per the manufacturer instructions (BPS Bioscience, Cat. #79802), using ADP-Glo ® Kinase Assay as a detection reagent and the luminescence was recorded using a microplate reader.

4.2.5. Cell cycle analysis and apoptosis assay. MCF-7 cells were seeded at 8×10^4 and incubated overnight at 37 °C and supplied with 5% CO $_2$. After 48 h of treatment, cell pellets were collected and centrifuged at 300 g for 5 min. For cell cycle analysis, cell pellets were fixed in 70% ethanol on ice for 15 min. The collected pellets were incubated with propidium iodide (PI) staining solution (50 $\mu\text{g ml}^{-1}$ PI, 0.1 mg ml^{-1} RNaseA and 0.05% Triton X-100) at room temperature for 1 h. Apoptosis detection was performed by FITC Annexin-V/PI kit (Becton Dickinson, Franklin Lakes, NJ, USA) following the manufacturer's protocol. The samples were analyzed by fluorescence-activated cell sorting (FACS) with a Gallios flow cytometer (Beckman Coulter, Brea, CA, USA) within 1 h from the staining. Data were analyzed using Kaluza v1.2 (Beckman Coulter).

4.3. Molecular docking

All the molecular modeling studies were carried out using Molecular Operating Environment (MOE-Dock, 2014.0901) software. All minimizations were performed with MOE until an RMSD gradient of 0.1 $\text{kcal mol}^{-1} \text{ \AA}^{-1}$ with MMFF94x force field and the partial charges were automatically calculated.

The X-ray crystallographic structures of EGFR complexed with erlotinib (PDB ID: 1M17), PI3K complexed with 6-(1*H*-pyrazolo [3,4-*b*]pyridin-5-yl)-4-pyridin-4-ylquinoline (PDB ID: 3L54) and mTOR complexed with 3-(4-morpholin-4-ylpyrido[3',2':4,5]furo [3,2-*d*]pyrimidin-2-yl)phenol (PDB ID: 4JT6) were downloaded from the protein data bank. The proteins were prepared for docking by removal of all ligands and water molecules that are not involved in the binding. One conserved water molecule involved in the co-crystallized ligand binding to EGFR binding site was kept. It is worth to mention that four chains make up the mTOR PDB file, and two of them, designated A and B, each include an original ligand whose binding modes to those two chains are noticeably similar. Therefore, only chain A was kept in order to perform molecular docking. All the proteins were then prepared for the docking study using Protonate 3D protocol in MOE with default options. The co-crystallized ligand was used to define the binding site for docking. Triangle Matcher placement method and London dG scoring function were used for docking.

4.4. *In silico* physicochemical properties, pharmacokinetics parameters and medicinal chemistry friendliness study

The physicochemical as well as the leadlike nature and medicinal chemistry friendliness of the promising compound **6a** were predicted using the free SwissADME web tool.

Conflicts of interest

The authors declared that there are no actual or potential conflicts of interest and have approved the article.

Acknowledgements

This research article was funded by NRC, Cairo, Egypt (2019–2021, ethical approval number: 19354) through the project no. 12010110 entitled “Comparative study of conventional and microwave assisted synthesis of some new *N*-heterocycles as anticancer agents”. The authors are grateful to Dr Eman S. Nossier, Department of Pharmaceutical Medicinal Chemistry and Drug Design, Faculty of Pharmacy (Girls), Al-Azhar University, Cairo, 11754, Egypt, for carrying out the molecular modeling study.

References

- 1 H. Sung, J. Ferlay, R. L. Siegel, M. Laversanne, I. Soerjomataram, A. Jemal and F. Bray, *Ca-Cancer J. Clin.*, 2021, **71**, 209–249.
- 2 Y. Xie, X. Shi, K. Sheng, G. Han, W. Li, Q. Zhao, B. Jiang, J. Feng, J. Li and Y. Gu, *Mol. Med. Rep.*, 2019, **19**, 783–791.
- 3 K. M. Keppler-Noreuil, V. E. R. Parker, T. N. Darling and J. A. Martinez-Agosto, *Am. J. Med. Genet., Part C*, 2016, **172**, 402–421.
- 4 J. E. Paes and M. D. Ringel, *Endocrinol. Metab. Clin. North Am.*, 2008, **37**, 375–387, viii–ix.
- 5 F. Xu, L. Na, Y. Li and L. Chen, *Cell Biosci.*, 2020, **10**, 54.
- 6 V. Papadimitrakopoulou, *J. Thorac. Oncol.*, 2012, **7**, 1315–1326.
- 7 A. F. Kassem, R. Z. Batran, E. M. H. Abbas, S. A. Elseginy, M. N. F. Shaheen and E. M. Elmahdy, *Eur. J. Med. Chem.*, 2019, **168**, 447–460.
- 8 N. A. Abdel Latif, R. Z. Batran, S. F. Mohamed, M. A. Khedr, M. I. Kobeasy, S. A. F. Al-Shehri and H. M. Awad, *Mini-Rev. Med. Chem.*, 2018, **18**, 1572–1587.
- 9 R. Z. Batran, D. H. Dawood, S. A. El-Seginy, T. J. Maher, K. S. Gugnani and A. N. Rondon-Ortiz, *Bioorg. Chem.*, 2017, **75**, 274–290.
- 10 R. Z. Batran, M. A. Khedr, N. A. Abdel Latif, A. A. Abd El Aty and A. N. Shehata, *J. Mol. Struct.*, 2019, **1180**, 260–271.
- 11 K. Venkata Sairam, B. M. Gurupadaya, R. S. Chandan, D. K. Nagesha and B. Vishwanathan, *Curr. Drug Delivery*, 2016, **13**, 186–201.
- 12 D. Srikrishna, C. Godugu and P. K. Dubey, *Mini-Rev. Med. Chem.*, 2018, **18**(2), 113–141.
- 13 F. F. Zhang, D. E. Haslam, M. B. Terry, J. A. Knight, I. L. Andrusis, M. B. Daly, S. S. Buys and E. M. John, *Cancer*, 2017, **123**, 2070–2079.
- 14 A. Puzskiel, G. Noé, A. Bellesoeur, N. Kramkimel, M.-N. Paludetto, A. Thomas-Schoemann, M. Vidal, F. Goldwasser, E. Chatelut and B. Blanchet, *Clin. Pharmacokinet.*, 2019, **58**, 451–467.
- 15 G. M. Keating, *Drugs*, 2017, **77**, 85–96.
- 16 N.-Y. Chen, Y.-L. Xie, G.-D. Lu, F. Ye, X.-Y. Li, Y.-W. Huang, M.-L. Huang, T.-Y. Chen and C.-P. Li, *Mol. Diversity*, 2021, **25**, 967–979.
- 17 R. Z. Batran, D. H. Dawood, S. A. El-Seginy, M. M. Ali, T. J. Maher, K. S. Gugnani and A. N. Rondon-Ortiz, *Arch. Pharm.*, 2017, **350**, 1700064.



- 18 N. A. Abdel Latif, R. Z. Batran, M. A. Khedr and M. M. Abdalla, *Bioorg. Chem.*, 2016, **67**, 116–129.
- 19 T. K. Mohamed, R. Z. Batran, S. A. Elseginy, M. M. Ali and A. E. Mahmoud, *Bioorg. Chem.*, 2019, **85**, 253–273.
- 20 E. Y. Ahmed, W. S. Elserwy, M. F. El-Mansy, A. M. Serry, A. M. Salem, A. M. Abdou, B. A. Abdelrahman, K. H. Elsayed and M. R. Abd Elaziz, *Bioorg. Med. Chem. Lett.*, 2021, **48**, 128258.
- 21 O. M. Abdelhafez, K. M. Amin, H. I. Ali, M. M. Abdalla and E. Y. Ahmed, *RSC Adv.*, 2014, **4**, 11569.
- 22 O. M. Abdelhafez, H. I. Ali, K. M. Amin, M. M. Abdalla and E. Y. Ahmed, *RSC Adv.*, 2015, **5**, 25312–25324.
- 23 O. M. Abdelhafez, E. Y. Ahmed, N. A. Abdel Latif, R. K. Arafa, Z. Y. Abd Elmageed and H. I. Ali, *Bioorg. Med. Chem.*, 2019, **27**, 1308–1319.
- 24 E. Y. Ahmed, N. A. Abdel Latif, M. F. El-Mansy, W. S. Elserwy and O. M. Abdelhafez, *Bioorg. Med. Chem.*, 2020, **28**, 115328.
- 25 R. Z. Batran, W. A. El-Kashak, S. M. El-Daly and E. Y. Ahmed, *ChemistrySelect*, 2021, **6**, 11012–11021.
- 26 R. Z. Batran, S. M. El-Daly, W. A. El-Kashak and E. Y. Ahmed, *Chem. Biol. Drug Des.*, 2022, **99**, 470–482.
- 27 H. A. Abuelizz, M. Marzouk, A. H. Bakheit, H. M. Awad, M. M. Soltan, A. M. Naglah and R. Al-Salahi, *Molecules*, 2020, **15**(25), 5944.
- 28 M. A. Abd-El-Maksoud, M. El-Hussieny, H. M. Awad, A.-T. H. Mossa and F. M. Soliman, *Russ. J. Gen. Chem.*, 2020, **90**, 2356–2364.
- 29 R. Abdel Elatif, M. Shabana, R. Mansour and H. M. Awad, *Egypt. J. Chem.*, 2020, **63**, 1713–1721.

